Number of Surface Sites and Turnover Frequencies for Oxide Catalysts

Israel E. Wachs

Operando Molecular Spectroscopy & Catalysis Laboratory

Department of Chemical & Biomolecular Engineering

Lehigh University

Bethlehem, PA 18015 USA

Abstract

Unlike for metal catalysts where selective chemisorption probes (H_2, O_2, CO and N_2O) have been successfully applied to count the number of active surface sites and allow determination of TOF values, the analogous situation for oxide catalysts has developed very slowly. The reason for the sluggish development of selective chemisorption probes for oxides is that the same chemisorption probes that work well with metals aren't compatible with oxides since these chemical probes weakly adsorb on oxides. Methanol, however, is a very reactive molecule that has been found to readily chemisorb on oxides and allows for quantitative determination of the number of active surface sites (Ns). In this mini-review, the determination of the number of active sites by methanol chemisorption is reviewed with examples for pure oxides (one-component oxides), supported oxides (submonolayer, monolayer and above monolayer) and bulk mixed oxides (surface enriched oxide present in submonolayer, monolayer and in excess of monolayer coverages).

Keywords: oxides, redox, acid, Ns, TOF

1. Introduction

Oxides find wide application as heterogeneous catalysts for numerous chemical reactions that require redox, acid or basic sites and their combinations [1]. Catalysts containing vanadia and molybdena are most commonly employed as oxidation catalysts (e.g., $CH_3OH \rightarrow H_2CO$ [2], $CH_3CH_3 \rightarrow CH_2{=}CH_2$ [3], $CH_3CH_2CH_3 \rightarrow CH_2{=}CHCH_3$ [4], $CH_2{=}CHCH_3 \rightarrow CH_2{=}CHCHO$ [5], n-$C_4H_{10} \rightarrow$ maleic anhydride [6], o-xylene $\rightarrow$ phthalic anhydride [7], $SO_2 \rightarrow SO_3$ [8,9], NO + $NH_3 \rightarrow N_2$ [10], etc.). Catalysts containing tungsta and phosphate are found in acid catalysts (n-$C_5H_{10} \rightarrow$ i-C_5H_{10} [11], $CH_3CH_2OH \rightarrow CH_2{=}CH_2$ [12], etc.). Catalysts containing MgO and ZnO are usually present in base catalysts [1,13–15]. Redox (VO_x and MoO_x), acidic (WO_x and PO_x) and basic (MgO_x and ZnO_x) sites are sometimes combined in oxides since the catalyzed reactions may require dual functional sites (redox-acid, redox-base or acid-base) [1,13,15,16].

Oxides can exist as either unsupported one-component bulk oxides, supported oxides and unsupported bulk mixed oxides [17]. Although one-component bulk oxides rarely find practical use, they serve as model oxide catalysts consisting of one bulk phase. Supported oxides consist of a two-dimensional metal oxide phase molecularly dispersed on the surface of a second oxide that acts as a support (e.g., Al_2O_3, SiO_2, SiO_2-Al_2O_3, ZrO_2, TiO_2, etc.). Bulk mixed oxides consist of two or more oxide components present in a single bulk phase (e.g., $Fe_2(MoO_4)_3$, $Bi_2(MoO_4)_3$, etc.), which makes them much more complex catalytic systems. The composition of bulk mixed oxides may deviate from stoichiometry and form an additional bulk oxide phase with the excess component (e.g., $MoO_3/Fe_2(MoO_4)_3$ for Mo/Fe > 1.5).

The development of titration methods (e.g., CO, H_2, O_2, O_2/H_2, N_2O, etc.) to count the number of exposed metallic surface sites of supported metals (e.g., Pt, Ru, Ir, etc.) has had a profound effect on the advancement of catalysis by supported metals starting in the 1960s [18]. Knowledge of the number of exposed surface sites (Ns) allowed for determining the reaction Turnover Frequency (TOF = reaction rate/Ns = molecules reacted per surface site per unit of time). This allowed for the first time quantitative comparison of catalytic results of the same or similar catalysts from different catalyst laboratories and comparison of supported metal catalysts and single crystal metals for a specified set of conditions. It demonstrated that reproducible catalytic results are obtainable from different laboratories and revealed the catalytic structure sensitivity and size dependence of supported metal particles.

The same titration approaches, however, are not successful with oxide catalysts because (*i*) CO only weakly adsorbs on metal oxides preventing titration of all the exposed surface sites, (*ii*) H_2 adsorption involves reaction with both surface and subsurface lattice oxygen, and (*iii*) O_2/N_2O do not adsorb on oxidized surfaces and O_2/N_2O adsorption on reduced surfaces proceeds by oxidation of both the surface and subsurface lattice oxygen vacancies [19]. Adsorption of H_2 and O_2 at subambient temperatures was attempted to prevent the participation of subsurface lattice oxygen and lattice oxygen vacancies, respectively, but was unsuccessful in preventing participation of the lattice oxygen atoms and oxygen vacancies [20]. A solution for this conundrum of determining the number of exposed surface sites present for oxides appeared in the literature in the 1980s [21–24]. The adsorption of small alcohols on dehydrated and/or evacuated oxides was found to be able to quantitatively and selectively count the number of active surface sites. Methanol has been observed to follow several chemisorption pathways on oxides: (*i*) CH_3OH + M-OH → M-OCH_3 + H_2O (M is metal cation site), (*ii*) CH_3OH + M-O-S → M-OCH_3 + S-OH (S is oxide support cation site) by breaking open heterobonds and (*iii*) CH_3OH + [*] → CH_3OH-[*] ([*] is a Lewis acid coordinatively unsaturated site) [25,26]. . There is no evidence that methanol chemisorbs by breaking open bridging M-O-M or reacts with terminal M=O bonds since the Mo(010) and V(010) basal planes contain these functionalities and these surface planes don't appear to extensively activate methanol for adsorption because they consist of coordinatively saturated sites [23]. These pioneering studies demonstrated that adsorption of CH_3OH, as well as other small alcohols, can count the number of exposed active surface sites of oxide catalysts and also provide structural reactivity information. For example, chemisorption of CH_3OH on anisotropic crystalline α-MoO_3 powder consisting of stacked molybdena sheets only takes place at the edge sites, which represents ~12% of the total exposed Mo sites [23], while chemisorption of CH_3OH on isotropic crystalline ß-MoO_3 powder that is uniform in all directions occurs at all exposed Mo sites resulting in a much higher methanol/Mo ratio [24]. Application of CH_3OH chemisorption on the isotropic bulk $Fe_2(MoO_4)_3$ mixed oxide powder revealed that for the crystalline iron molybdate phase the number of exposed sites was increased by as much as a factor of ~4x, which was proposed to account for the greater methanol oxidation activity of crystalline $Fe_2(MoO_4)_3$ compared to crystalline α-MoO_3. This conclusion is consistent with the similar HCHO desorption temperatures (Tp) from the oxidation of chemisorbed methanol on α-MoO_3 (~205°C) and $Fe_2(MoO_4)_3$ (~209°C) during CH_3OH-TPSR [27].

The IR C-H vibrations of the surface CH_3OH* and surface CH_3O* species were found to be diagnostic of the identity of the oxide surface site that these surface intermediates are coordinated [26]. For example, (*i*) chemisorption of methanol on weak Lewis acid sites adjacent to basic sites (Bi_2O_3, Fe_2O_3, NiO, ZnO and ZrO_2) results in dissociated surface CH_3O* intermediates (relatively low frequency C-H vibrations at ~2800-2910 cm^{-1}) and (*ii*) chemisorption of methanol on strong Lewis-acid sites (Al_2O_3, MoO_3, Nb_2O_5, SiO_2, WO_3, V_2O_5, TiO_2 and CeO_2) produces dissociated surface CH_3O* species with higher C-H stretching frequencies (~2830/~2930 cm^{-1}) as well as intact surface CH_3OH* at the Lewis acid coordinatively unsaturated sites with higher C-H stretching frequencies (~2850/~2950 cm^{-1}). Furthermore, the IR C-O vibrations of surface methoxy in the 1050-1150 cm^{-1} range also inform about the identity of the anchoring surface site and the number of coordinating cations (atop, doubly bridging or triply bridging), and are also sensitive to the cation oxidation state [28]. Thus, *in situ* IR analysis of chemisorbed methanol on oxides can potentially distinguish between the different elements present in the outermost surface layer of mixed oxides and provides surface compositional information in a methanol environment. This is especially the situation when one element is a strong Lewis acid and one element is a weak Lewis acid (e.g., MoO_x and FeO_x, respectively) [27]. This is very important for determining if a complete monolayer of one surface oxide is present for a bulk mixed oxide catalyst that will be addressed below. When the IR studies are performed in transmission mode and the extinction coefficients are determined, the amounts of each chemisorbed methanol species can be directly quantified [28]. Furthermore, the strong interaction of methanol with oxide surfaces also displaces other surface species (e.g., H_2O, etc.) during methanol adsorption and reaction, which suggests similar surface structures are present during methanol chemisorption and methanol oxidation reaction conditions [24].

In spite of the above advances in counting exposed surface sites of oxides with small alcohols about four decades ago, this methodology has not been commonly applied to catalysis by oxides. Consequently, most of the catalysis literature for oxides just presents the data as qualitative selectivity *vs.* conversion plots rather than determining the TOF values, which doesn't allow determining if the changes in activity are from the number of active surface sites (Ns) or specific catalytic activity (TOF). This represents a missed opportunity by the catalysis community studying oxide catalysts. An exception to this trend is the determination of number of surface sites for supported oxides (e.g., V_2O_5, MoO_3, etc.) where the supported oxide phase is completely dispersed below monolayer coverage on a high surface area oxide support (e.g., Al_2O_3, SiO_2, etc.) and, thus, the number of active sites at monolayer or lower coverage is known. In the absence of reported TOF values for unsupported oxide catalysts, it is not easy to compare the specific catalytic activity between different laboratories, different catalysts and the influence of synthesis methods and promoters. This mini-review will examine the available data in the heterogeneous catalysis literature about the surface site density (number of exposed active sites) and the corresponding TOF values for methanol oxidation by different types of oxide catalysts: (*i*) unsupported pure bulk oxides (one-component oxides), (*ii*) supported oxides (one-component and multicomponent) and (*iii*) unsupported bulk mixed oxides. The number of reported studies of methanol chemisorption studies on oxides is rather limited and in most cases are not accompanied by additional characterization studies [23,26,28,29]. Consequently, the current paper will primarily focus on the extensively characterized oxide catalysts reported by the Wachs laboratory to allow for a consistent set of well-defined oxide catalysts (dehydrated in an O_2 environment at elevated temperatures (350°C), chemisorption of CH_3OH at 100°C) and the additional fact that almost all the publications on quantitative methanol chemisorption since 2000 have come from the Wachs laboratory. Comparisons with published findings from other groups will also be made when such data are available.

2. Unsupported One-Component Oxides

As mentioned in the introduction, the early studies in the 1980s mostly determined the number of exposed active surface sites on one-component oxides and most of the studies primarily focused on the type of methanol adsorption isotherm (Langmuir, Elovich/Temkin or BET type II involving multilayer adsorption): ZnO [21,30–32], MoO_3 [33,34], Al_2O_3 [35], MgO [32,36], TiO_2 [37,38], Cr_2O_3 [39], CeO_2 [40] and ZrO_2 [41], as well as IR studies investigating the nature of the surface CH_3O^*/CH_3OH^* species [42–46]. Comparison of the reported values for the CH_3OH/M ratios is complicated by the different experimental conditions among these studies: (*i*) oxide single crystals and powders, (*ii*) vacuum conditions and high pressures (with different CH_3OH partial pressures), and (*iii*) different methanol chemisorption temperatures. Badlani and Wachs extended such methanol chemisorption measurements by thermogravimetric analysis to approximately three dozen one-component oxides as shown in Table 1, allowing for a side-by-side comparison in the same TGA system, same oxidation treatment and same chemisorption conditions [47]. The one-component oxides were either purchased or prepared from their precursors by calcination with details previously provided [47]. The oxides were initially exposed to flowing 20% O_2/He at 350°C for 1 hr. to desorb moisture, remove surface impurities and oxidize the oxides to the maximum extent. Importantly, an adsorption temperature of 100°C was selected to minimize the presence of weakly physisorbed CH_3OH molecules that complicated earlier studies performed at ~25°C since these studies also contained condensed methanol (boiling point of methanol is 64.7°C) that affected the determined CH_3OH/M values [29,33]. The number of active surface sites for methanol chemisorption on oxides can be quantitatively determined via several methods: (*i*) thermal gravimetric analysis [23], (*ii*) *in situ* transmission IR of chemisorbed methanol species [26], and (*iii*) analysis of reaction products generated during Temperature Programmed Surface Reaction (TPSR) spectroscopy [27]. Importantly, methanol chemisorption and reaction of surface CH_3O^*/CH_3OH^* readily take place on all oxides indicating that methanol is a reactive chemical probe that can count the exposed active surface sites on oxides [47].

Table 1. Number of active surface sites derived from CH_3OH chemisorption on pure oxides at 100°C as determined by TGA after a calcination pretreatment at 350°C [47]. Number of active sites corrected by 3x CH_3OH/MO_x since only ~1 out of ~3 surface MO_x sites becomes titrated by CH_3OH [26].

Oxide	**Number of Active Surface Sites (Ns) (3 x CH_3OH/M x 10^{15} sites/cm^2)**
La_2O_3	6.1
MgO	4.1
Cr_2O_3	2.2
NiO	1.2
Al_2O_3	0.99
CaO	0.97
Ag_2O*	0.94
Y_2O_3	0.89
Sb_2O_3*	0.88
Ta_2O_5	0.83
PdO*	0.77
SrO	0.77
CeO_2	0.76
TeO_2	0.74
Ga_2O_3	0.74
BaO	0.71
Fe_2O_3	0.71
TiO_2	0.67
CuO*	0.65
P_2O_5	0.65
Rh_2O_3*	0.63
PtO*	0.56
In_2O_3	0.49
Co_3O_4	0.49
Nb_2O_5	0.47
HfO_2	0.47
WO_3	0.42
Bi_2O_3	0.38
Mn_2O_3	0.29

Sn_2O_3	0.29
ZrO_2	0.20
MoO_3	0.14
V_2O_5	0.13
ZnO	0.05
SiO_2	0.041

*These oxides reduced at 100°C during methanol chemisorption and an adsorption temperature of 50°C was found to prevent reduction. The reported number of sites at 50°C were then extrapolated to 100°C by comparison with the temperature dependence of Ns for non-reducible oxides [47].

The number of active surface sites for the one-component oxides was quantitatively measured with a TGA by methanol chemisorption at 100°C and the surface density of active sites is presented in Table 1, after the correction applied for the more reducible oxides. The number of active surface sites varied from a low value of ~0.04 x 10^{15} sites/cm^2 to a high value of ~6 x 10^{15} sites/cm^2 with the most common value being ~0.7 x 10^{15} sites/cm^2. The much lower Ns surface density values for oxides compared to metals (~1.2 x 10^{15} sites/cm^2) [18] reflects the lower number of exposed active sites for oxides associated with the lower surface cation density [26]. The very low Ns values (0.04-0.15 x 10^{15} sites/cm^2) reflect the anisotropic nature of ZnO, MoO_3, V_2O_5, which indicates the presence of low activity exposed surface planes, and the very low reactivity of the surface sites on SiO_2. The very high values for La_2O_3 (~6 x 10^{15} sites/cm^2), MgO (~4 x 10^{15} sites/cm^2), and Cr_2O_3 (~2 x 10^{15} sites/cm^2) reflect their ability to readily form multilayers of carbonates during methanol chemisorption at 100°C. Only one publication for methanol chemisorption on crystalline Ga_2O_3 polymorphs employed the same treatment as used for collecting the data in Table 1 and reported a value of $Ns_{,Ga2O3}$ = 0.36 x 10^{15} sites/cm^2, which is within a factor of 2 of the value reported in Table 1 for Ga_2O_3 [48]. The other reported quantitative methanol chemisorption studies usually applied an evacuation treatment, performed methanol chemisorption at room temperature and employed IR spectroscopy for quantification. The reported $Ns_{,CeO2}$ = 0.84 x 10^{15} sites/cm^2 value [49] is close to the value of $Ns_{,CeO2}$ = 0.76 x 10^{15} sites/cm^2 value given in Table 1. The reported $Ns_{,ZrO2}$ = 0.81 x 10^{15} sites/cm^2 value [49] is 4x greater than that reported for ZrO_2 in Table 1. Some of this difference may be related to the presence of physically chemisorbed CH_3OH present in the reported study [49]. The reported $Ns_{,MgO}$ = 0.57 – 0.98 x 10^{15} sites/cm^2 value [49], however, is close to that anticipated for monolayer coverage and reveals that methanol chemisorption at 25°C suppresses the multilayer chemisorption at 100°C that is reported in Table 1 for MgO. This suggests that methanol chemisorption at ~25°C results in more representative Ns values for strong basic oxides. In summary, methanol chemisorption is a good quantitative chemical probe for determining the number of active surface sites with a value of ~0.7 x 10^{15} sites/cm^2 being representative of isotropic oxides and much lower Ns values for anisotropic oxides with inactive surface planes due to coordinative saturation of the sites. Consequently, if the number of active surface sites has not been measured with methanol chemisorption for isotropic one-component oxides, the value of Ns = ~0.7 x 10^{15} sites/cm^2 can be applied as a first approximation for determining TOF values.

Knowledge of the Ns values for the pure oxides allows determining their corresponding TOF values for methanol oxidation at 300°C that is shown in Figure 1 [47]. The TOF values for the pure oxides are separated into two categories since surface redox sites primarily produce HCHO (F: formaldehyde) with small amounts of CH_3OOCH (M: methylformate) and $(CH_3O)_2CH_2$ (DMM: dimethoxymethane), and surface acid sites form CH_3OCH_3 (DME: dimethyl ether). Methanol conversions were kept low (<10%) in order to minimize secondary reactions. The specific activity findings reveal that the methanol oxidation TOF_{redox} values vary almost seven orders of magnitude from ~10^{-3} to ~10^4 s^{-1}. The highest TOF_{redox} value is exhibited by PtO (~10^4 s^{-1}) and the other precious metal oxides (PdO, Rh_2O_3 and Ag_2O) also possess high TOF_{redox} values (~10^1-10^2 s^{-1}). The transition metal oxides (Cr_2O_3, Co_3O_4 and Mn_2O_3) are also quite active with TOF_{redox} values below those of the precious metal oxides (~10^1 s^{-1}). The influence of heat and mass transfer on these more active oxides is minimal as evidenced by the scaling of the TOF values with the surface CH_3O^*/CH_3OH^* decomposition temperatures during temperature programmed surface reaction (TPSR) spectroscopy, as will be discussed below [47]. The methanol oxidation TOF_{acid} values vary almost three orders of magnitude from ~10^{-4} to ~10^{-1} s^{-1}, with SiO_2 having a TOF_{acid} of ~10^{-4} s^{-1}. The highest TOF_{acid} values are exhibited by Al_2O_3 and Ga_2O_3, and are followed by Fe_2O_3, P_2O_5, WO_3 and V_2O_5. The TOF_{acid} values for the more basic oxides are essentially zero (e.g., Mg, Sr, Ca, Ba, Y, Hf, Ce, Mn, Zn, Bi, etc.). Note that the same catalytic oxide can exhibit both redox and acid active surface sites with the redox sites generally much more active than acid sites.

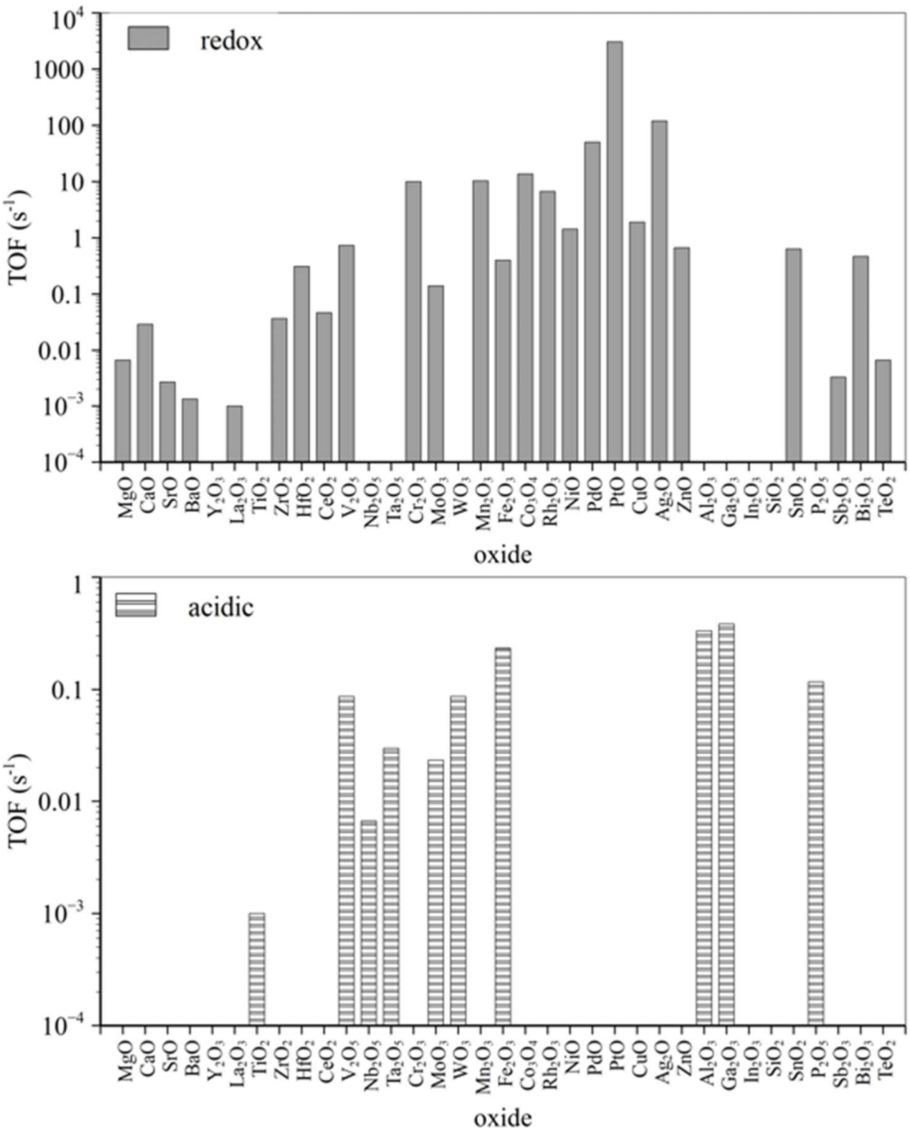

Figure 1. Methanol oxidation TOF values for pure one-component oxides at 300°C. Replotted from the data from ref. [47]. Note, the above TOF values have been corrected for the CH_3OH/MO_x stoichiometry of ~1/3, which reduces the previously reported TOF values by a factor of 3 [47].

Having such an extensive collection of TOF values for methanol oxidation by the one-component oxides provides an opportunity to examine how the TOF values correlate with different properties of the oxides [47]. For the most selective redox oxides (>85% selectivity: Ag_2O, PdO, Mn_2O_3, CuO, NiO, V_2O_5, SnO_2, HfO_2, MoO_3, CeO_2, ZrO_2, CaO, Sb_2O_3 and TeO_2), the steady state TOF values were plotted versus (*i*) bulk heat of formation of the oxides, (*ii*) H_2-TPR reduction temperature, (*iii*) isotopic O_2 exchange rate constant, and (*iv*) surface methoxy decomposition temperature. No clear correlations were found between the methanol oxidation TOF_{redox} values and (*i*) metal oxide bulk heat of formation (R^2 = 0.2-0.3 for linear, log and 2nd-order polynomial fits to the data points), (*ii*) H_2 reduction temperature (that proceeds through breaking of H-H bonds and formation of surface hydroxyls) and (*iii*) isotopic O_2 exchange rate constant[50]. Furthermore, it also demonstrates that H_2-TPR is not an appropriate chemical probe for reflecting the rates of oxidation reactions, which is commonly applied in the literature, and that a more appropriate probe is the reactant actually involved in the redox reaction (e.g., CH_3OH in the present case for methanol oxidation). The steady state TOF_{redox} values do nicely inversely correlate with the decomposition temperatures of the surface methoxy/methanol species (the higher the decomposition temperature of the surface methoxy/methanol, the lower the TOF_{redox} value ($R^2 = 0.96$ for linear fit to the data points)) [47]. This indicates that (*i*) the rate-determining step is dominated by the breaking of the surface methoxy/methanol C-H bond and (*ii*) the more stable the C-H bond, the lower the steady state TOF_{redox} value for methanol oxidation [50]. A similar inverse relationship was also found for HCOOH oxidation on pure oxides [51]. In both cases the left side of a "volcano" curve was not present suggesting that the thermal stability of the surface intermediate determines the TOF value.

The selectivity in redox reactions has been proposed to be controlled by the mobility of oxygen atoms in the catalyst lattice: high oxygen mobility leads to low selectivity because of over-oxidation of the reaction products and low oxygen mobility leads to high selectivity because of limited over-oxidation of the reaction products [52,53]. In spite of this popular hypothesis, supporting data were never provided. The plot of redox selectivity for methanol oxidation *vs*. the rate of isotopic $^{16}O_2$–$^{18}O_2$ exchange gives rise to an uncorrelated, random plot [47,54] that doesn't support this hypothesis. The same conclusion is reached when comparing the oxide catalysts that are 100% selective towards redox products during methanol oxidation with their bulk M-O heats of formation (Ag_2O (7 kcal/mol), PdO (20 kcal/mol), CuO (38 kcal/mol), TeO_2 (39 kcal/mol), Sb_2O_3 (56 kcal/mol), SnO_2 (69 kcal/mol) and HfO_2 (133 kcal/mol)) since their bulk M-O heats of formation vary over an order of magnitude while the selectivity does not change [47]. Additionally, the redox selectivity also does not depend on the specific activity of the metal oxide catalytic site since the TOF_{redox} values vary by six orders of magnitude and the selectivity to redox products remains 100% [47]. It appears, thus, that the hypothesis that oxygen mobility in oxides controls the selectivity of redox reactions catalyzed by oxides is not supported by the methanol oxidation reaction. It would not be possible to address this important issue without independently determining the Ns and TOF values that were lacking in previous redox catalytic studies by oxides.

The methanol chemical probe reactions, thus, inform about the relative TOF_{redox} and TOF_{acid} values of the pure oxides. Similar TOF_{redox} and TOF_{acid} trends were also found for isopropanol reactions on the pure oxides forming acetone and propylene products, respectively [55]. Although such data for other chemical reactions by pure oxides have still not appeared in the literature, it is anticipated that similar trends will also be found. Such additional data for pure oxides are highly desired for establishing a fundamental understanding of the intrinsic kinetics of each pure oxide catalyst for other reactions since such information can guide the rational design of bulk and supported mixed oxide catalysts.

3. Supported Oxides

Supported oxide catalysts are formed by deposition of an active oxide on a high surface area oxide support (e.g., vanadia on TiO_2). In such a situation, the active component is present as a dispersed surface oxide phase (e.g., surface VO_x sites) on the oxide support (TiO_2). Five scenarios can occur for supported oxide catalysts: (*i*) surface oxide phase is below monolayer coverage, (*ii*) supported multilayers (M_1O_x/M_2O_x/Support), (*iii*) surface oxide phase is present as a complete monolayer on the oxide support, (*iv*) surface oxide monolayer consists of more than one element (e.g., VO_x and WO_x sites), and (*v*) supported oxide phase exceeds monolayer coverage with the excess oxide forming crystalline nanoparticles (NPs) (e.g., V_2O_5) on top of the surface oxide monolayer.

(*i*)_**Surface oxide phase below monolayer coverage.** Below monolayer coverage, both the sites from the surface oxide phase and the oxide support will be exposed and methanol will chemisorb on both sites. If the IR or Raman vibrations of the surface methoxy/methanol species are different from the surface oxide phase and the oxide support, then it will be possible to quantitatively determine the number of surface sites associated with the surface phase and the oxide support.

Redox sites. Such a scenario typically occurs for oxides dispersed on SiO_2 supports because of the low reactivity of the surface Si-OH hydroxyls towards anchoring of oxides. For example, the poor dispersion of oxides on a SiO_2 support only yields a maximum surface VO_x coverage corresponding to ~33% of monolayer (0.2×10^{15} cm^{-2}) of isolated surface VO_x sites indicating that both surface VO_x and Si-OH sites are exposed [56]. Exposure to methanol reveals that both surface V-OCH_3 (2832 and 2930 cm^{-1}) and Si-OCH_3 (2856 and 2956 cm^{-1}) intermediates are present. The redox surface V-OCH_3 intermediates readily decompose to HCHO as the temperature is raised while the surface Si-OCH_3 intermediates are spectator species and sluggishly decompose to CO_x and DME at higher temperatures. Combining the vibrational spectroscopy with Temperature Programmed Surface Reaction (TPSR) spectroscopy allows quantification of the number of surface V-OCH_3 and Si-OCH_3 intermediates in this catalyst with submonolayer coverage of surface VO_x sites. The TOF value for CH_3OH oxidation by the supported VO_x/SiO_2 catalyst at 230°C is quite low (1.3×10^{-4} s^{-1}) because of the retardation of the redox property of the surface VO_x site by formation of the stable bridging V-O-Si bond. Furthermore, the TOF_{redox} value is independent of surface VO_x coverage reflecting that only one surface VO_x site is involved in the oxidation of CH_3OH to HCHO and H_2O.

Acid sites. Surface WO_x sites possess acidic character and supported WO_x catalysts have been investigated for CH_3OH dehydration to CH_3OCH_3 as a function of surface WO_x coverage on oxide supports [51]. For the supported WO_x/ZrO_2 catalyst, the TOF_{acid} at 230°C increases about an order of magnitude with surface WO_x coverage in the submonolayer region, reflecting the stronger acidity of the surface WO_x sites present at higher surface coverage. The stronger acidity with surface WO_x coverage is related to preferential anchoring of WO_x at basic surface hydroxyls (Zr-OH) at lower coverage [57,58].

(*ii*) **Supported Multilayers (M_2O_x/M_1O_x/Support)**

Multilayer phases, M_2O_x/M_1O_x/Support where one oxide is anchored to the oxide support (M_1) and a second oxide (M_2) is anchored at the first oxide can be present for some supported oxide systems. Most of the reported multilayer catalyst studies have focused on the SiO_2 support since the second oxide is selectively anchored at the first surface oxide [59–61]. This occurs because of the (*i*) the generally weak interaction between oxides and the silica surface that favors anchoring of the second oxide (M_2) at the surface M_1-OH sites of the first oxide and (*ii*) the first oxide consumes the reactive Si-OH anchoring sites forming the surface M_1-OH anchoring sites. For SiO_2-based materials, the multilayer M_2O_x/M_1O_x/Support catalyst systems correspond to the case of surface oxide phase below monolayer coverage because the low reactivity of the Si-OH sites prevents formation of a complete surface oxide monolayer. Methanol chemisorption studies on multilayer non-SiO_2 supports have not received attention and, thus, will not be addressed.

Redox sites. The methanol oxidation data reveal that the M_1O_x sites (M_1 = Ti, Zr and Al) in the first layer increase the TOF_{redox} of surface VO_x in the second layer by factors of ~10^1-10^2 [59–61]. Analogous increases in methanol oxidation TOF_{redox} of surface MoO_x and ReO_x sites anchored at the surface M_1O_x sites (M_1 = Ti, Zr and Al) in bilayered $M_2O_x/M_1O_x/SiO_2$ catalysts have also been found [62]. This observation exemplifies the importance of the anchoring oxide support cations on the specific catalytic redox performance of surface MO_x sites.

Acid Sites. In contrast to the redox sites, the presence of M_1O_x sites (M_1 = Ti and Zr) in the first layer decrease the catalytic activity of acid surface WO_x sites present in the second layer for methanol dehydration to the DME product [62]. Again, the TOF_{acid} of the acidic surface WO_x sites are tuned by the anchoring oxide support cations.

(*iii*) Monolayer of surface oxide phase (one element). When a monolayer of surface oxide is present it completely covers all the exposed oxide support surface sites. The formation of a complete monolayer needs to be independently confirmed and is usually achieved with spectroscopy (e.g., Raman to confirm maximum surface oxide dispersion without formation of crystalline NPs, IR to confirm that all surface hydroxyls of the oxide support have been titrated by the surface oxide phase and that methanol is not bonded to the oxide support, and Low Energy Ion Scattering (LEIS) to monitor the elemental composition of the outermost surface layer). For a complete surface oxide monolayer without exposed oxide support sites, chemisorption of methanol will directly provide the number of active surface oxide sites and the TOF values will indicate the specific reactivity of the surface oxide sites in the monolayer.

Redox sites. This scenario is found for most non-SiO_2 supported oxide phases that readily form monolayer coverage of surface oxides (e.g., Al_2O_3, Nb_2O_5, ZrO_2, TiO_2, CeO_2, etc.) [63]. For example, a complete surface VO_x monolayer forms on Al_2O_3 (0.8 x 10^{15}/cm^2) and *in situ* IR only exhibits the vibrations of surface V-OCH_3 species (2830 and 2930 cm^{-1}) [26]. The TOF_{redox} value at 230°C for VO_x/Al_2O_3 is 2 x 10^{-3} s^{-1} which is much higher than for VO_x/SiO_2 (1.3 x 10^{-4} s^{-1}) reported above, reflecting the weaker bridging V-O-Al bond [64].

Acid sites. For monolayer surface WO_x coverage for the supported WO_x/ZrO_2 catalyst, as well as other supported WO_x catalysts such as WO_x/TiO_2 and WO_x/Nb_2O_5, the TOF_{acid} for methanol dehydration is ~10^{-2}-10^{-3} s^{-1} at 230°C [65]. The TOF_{acid} at monolayer surface WO_x coverage is also affected by the oxide support (WO_x/TiO_2 > WO_x/Nb_2O_5 > WO_x/ZrO_2) with the WO_x/TiO_2 catalyst being an order of magnitude more active.

(*iv*) **Monolayer of surface oxide phase (more than one element).** When two or more oxides are present in the surface oxide monolayer, the situation is more complex. Methanol will chemisorb at all the available surface oxide sites and spectroscopic characterization will need to be employed to distinguish between the methanol molecules chemisorbed at each of the different surface oxide sites. If the IR vibrations of the surface methoxy/methanol species are different on the two different surface oxide sites, then it will be possible to quantitatively determine the number of each surface site. This would be important to determine in a scenario where only one of the surface sites is active and the second surface site is inactive for the reaction being investigated, and would prevent over counting of the active surface sites. If the surface methoxy/methanol vibrations on the two surface oxide sites are identical, then it will not be possible to distinguish between the two surface oxide sites with IR or Raman spectroscopy. When the surface composition of the two oxide sites is known from the composition of the synthesis step, then to a first approximation it may be assumed that the surface methoxy/methanol associated with A sites is just:

surface methanol on A = total chemisorbed methanol x (# surface A sites/# surface A+B sites) (1).

Methanol-TPSR could provide more direct information about the number of A-OCH_3 and B-OCH_3 sites if the kinetics of the two surface intermediates are different. The situation, obviously, becomes much more complex when more than two different surface oxides are present in the surface oxide monolayer. An example of methanol chemisorption on a supported KO_x-VO_x/Al_2O_3 mixed oxide monolayer shows distinct Raman vibrational bands from basic surface K-OCH_3 and IR bands from redox surface V-OCH_3 species [66]. For mixed oxide monolayers where both surface oxides are strongly acidic (e.g., VO_x-WO_x/TiO_2), the surface methoxy C-H vibrations will essentially be indistinguishable for V-OCH_3 and W-OCH_3.

(*v*) **Supported oxide phase exceeds monolayer coverage with the excess oxide forming crystalline nanoparticles (NPs) on top of the surface oxide monolayer.** Above monolayer coverage, the same oxide element is present in both the surface oxide phase and the excess oxide making up the crystalline NPs residing on top of the monolayer phase. In such a situation, it will not be possible to distinguish between the chemisorbed CH_3O^*/CH_3OH^* on the surface oxide monolayer and the crystalline NPs because the IR vibrations from both sites will be identical since they are coordinated to the same element. Methanol chemisorption, however, will still provide the total number of the active surface oxide sites in the catalyst.

Redox sites. The number of chemisorbed surface methanol intermediates on supported VO_x/Al_2O_3 attains a maximum at surface VO_x monolayer coverage and slightly decreases above monolayer coverage (at ~1.5 monolayer equivalent) when modest amounts of crystalline V_2O_5 NPs are residing on top of the surface VO_x monolayer [64]. The corresponding TOF_{redox} for methanol oxidation at 230°C is relatively constant at ~6 x 10^{-3} s^{-1} at both monolayer and slightly above monolayer surface coverage indicating that the crystalline V_2O_5 NPs on Al_2O_3 don't significantly contribute to the number of active sites and the corresponding TOF_{redox} value for methanol oxidation.

Acid Sites. For the supported WO_x/ZrO_2 catalyst, as well as other supported WO_x catalysts such as WO_x/TiO_2 and WO_x/Nb_2O_5, the number of chemisorbed surface CH_3O^*/CH_3OH^* intermediates significantly decreases when ~2-3 monolayer equivalents of WO_x are deposited on the support [65]. This trend occurs because of the decreased accessibility of the surface WO_x sites due to the monolayer being covered by a significant amount of WO_3 nanoparticles. The TOF_{acid} value of these catalysts with excess tungsten oxide for methanol dehydration, however, further increases by an order of magnitude up to ~3 x 10^{-2} s^{-1} reflecting the presence of stronger acid sites on the crystalline WO_3 nanoparticles than the surface WO_x monolayer (as low as ~1 x 10^{-3} s^{-1}).

(*vi*) **Other supported oxide systems.** Methanol chemisorption can also be applied to determine the nature and number of active surface sites for other types of supported oxide catalyst systems such as MO_x/zeolites and MO_x/molecular sieves since they are no different than the above discussed supported oxide catalyst systems. For example, (*i*) V-silicalite can be thought of as analogous to supported VO_4/SiO_2, (*ii*) ZSM-5 can be thought of as supported AlO_4/SiO_2 and (*iii*) MO_x/ZSM-5 can be thought of as a supported $M_2O_x/AlO_4/SiO_2$ multilayered oxide [67]. Granted that the long range environment around the catalytic active site (MO_x) will be different among these systems, but the local environments are remarkably similar. Thus, methanol chemisorption can also be used to quantify the number of sites and the TOF values for such supported oxide catalyst systems. Polyoxometallates (POMs) represent another class of supported mixed oxides, but methanol chemisorption cannot be applied for these systems since POM aggregates both absorb methanol in the intermolecular spaces as well as chemisorb methanol on the external sites, which doesn't allow straightforward quantification of the external sites [68].

The methanol chemical probe reactions of supported metal oxide catalysts, with the assistance of IR spectroscopy and TPSR, can inform about the (*i*) surface CH_3O^*/CH_3OH^* coordination sites, (*ii*) CH_3O^*/CH_3OH^* surface chemistry, (*iii*) quantify the number of active surface sites below monolayer coverage and (*iv*) determine the number of available exposed sites above metal oxide monolayer coverage. Although the number of sites below monolayer coverage can be independently determined with other methods, the quantification of the number of available exposed sites above monolayer coverage has previously been quite elusive. An opportunity exists in extending the determination of number of surface sites with methanol chemisorption to determine the TOF values of other catalytic reactions.

4. Unsupported Bulk Mixed Oxides

Unsupported bulk mixed oxides consist of two or more oxide elements (e.g., iron molybdate, iron vanadate, zirconium tungstate, etc.) and it is critical to determine the number of active oxide sites present on the outermost surface layer in order to be able to calculate the TOF values. Although methanol chemisorption will provide the total number of sites, it is important that the chemisorption reflect the number of active surface sites since for bulk mixed oxides all the oxide elements may be present on the outermost surface layer. Three cases can occur for bulk mixed oxides: (*i*) surface coverage of the enriched oxide is below monolayer and more than one oxide element is exposed in the outermost layer, (*ii*) one of the oxides surface segregates to form a complete monolayer, and (*iii*) surface coverage of the enriched oxide exceeds monolayer and crystalline oxide NPs form on top of the monolayer. For all scenarios, methanol chemisorption will provide the total number of active surface oxide sites. However, the chemisorption must be combined with spectroscopic characterization to confirm the elemental surface composition and structural arrangements in these three scenarios. *In situ* LEIS surface analysis can confirm that monolayer surface coverage of one of the oxides has been achieved because of its unique sensitivity to the elements in the outermost surface layer. Corresponding XPS surface analysis will not be that informative since XPS typically analyzes ~3-10 layers and will have difficulty distinguishing between the oxides in the outermost surface layer and the subsurface layers. *In situ* Raman will generally inform if crystalline NPs are present because of the strong Raman scattering from crystalline oxide phases. *In situ* IR will confirm the nature of the surface oxide elements if the surface CH_3O*/CH_3OH* species vibrate differently when coordinated at each of the oxide elements. For example, *in situ* IR of methanol chemisorption on bulk $Zr_xCe_{1-x}O_2$ revealed that the surface composition is identical to the bulk composition [28].

(*i*)_Coverage of surface enriched oxide below monolayer.

Redox Sites. The *in situ* IR spectra for methanol chemisorbed on the bulk $Fe_2(MoO_4)_3$, MoO_3 and Fe_2O_3 phases are presented in Figure 2 [27]. Chemisorption of CH_3OH on Fe_2O_3 gives rise to two strong IR peaks at 2924 and 2820 cm^{-1} that are characteristic of the C-H stretches from surface Fe-OCH_3 species. The small shoulders at ~2950 and ~2850 cm^{-1} originate from the C-H stretches of Lewis site bound intact surface CH_3OH* species. Chemisorption of methanol on MoO_3 also gives rise to IR bands for both surface Mo-OCH_3 (2938 and 2832 cm^{-1}) and Lewis site bound intact surface CH_3OH* species (2958 and 2856 cm^{-1}), with the peaks for the latter much stronger. The IR vibrational peaks from the surface Mo-OCH_3 and Fe-OCH_3 species differ by ~10-14 cm^{-1} allowing distinguishing between the surface CH_3O* and intact CH_3OH* species coordinated to the surface Mo and Fe sites. LEIS surface analysis of the stoichiometric bulk iron molybdate (Mo/Fe = 1.5) mixed oxide reveals that the surface is enriched with MoO_x sites that do not form a complete monolayer since exposed Fe sites are also detected [26]. The *in situ* IR spectrum after methanol chemisorption on stoichiometric bulk iron molybdate (Mo/Fe = 1.5) is also shown in Figure 2 and comparison with the IR spectra of the bulk MoO_3 and Fe_2O_3 oxides reveals that both the surface CH_3O* species and intact surface CH_3OH* are predominantly coordinated to the surface Mo oxide sites since only weak shoulder bands from surface Fe-OCH_3 species are present (2924 and 2820 cm^{-1}). Methanol chemisorbed on a catalyst containing a surface MoO_x monolayer on Fe_2O_3, which was confirmed with LEIS surface analysis, exhibits essentially the same strong IR peaks (see spectra for supported 2.3% MoO_3/Fe_2O_3 in Figure 2), but the weak bands from surface Fe-OCH_3 species (2924 and 2820 cm^{-1}) are not present. Interestingly, this also reveals that methanol preferentially chemisorbs at the redox active surface MoO_x sites even when some redox inactive exposed FeO_x sites are exposed below monolayer (FeO_x sites possess acidic character and form DME while MoO_x sites are redox sites primarily producing the desired HCHO product). Methanol chemisorption on the stoichiometric bulk $Fe_2(MoO_4)_3$ crystalline phase gives the total number of redox active sites as 1.1 x 10^{15} sites/cm^2 and a TOF_{redox} of 0.03 s^{-1} for methanol oxidation at 230°C. The surface density of the active surface MoO_x sites for the anisotropic MoO_3 crystalline phase is 0.16 x 10^{15} sites/cm^2, which is much lower than the isotropic $Fe_2(MoO_4)_3$ crystalline phase indicating that isotropic mixed oxide phases possess much higher surface density of active sites than anisotropic oxides as previously reported [24]. The similar Tp values for methanol oxidation to HCHO for bulk MoO_3 and stoichiometric $Fe_2(MoO_4)_3$ also reveals that the surface MoO_x sites in both phases possess the same specific redox activity. The surface enrichment of MoO_x in bulk molybdates and VO_x in bulk vanadates accounts for the similar TOF_{redox} and selectivity values during methanol oxidation by bulk molybdate and bulk vanadate mixed oxide catalysts, respectively [69,70]. It seems that, in general, the bulk molybdate and vanadate mixed oxides are highly surface enriched in the active surface MoO_x and VO_x sites that minimize side reactions from the counter cations (e.g., Fe, Ni, Bi, etc.) to unselective products [69,71].

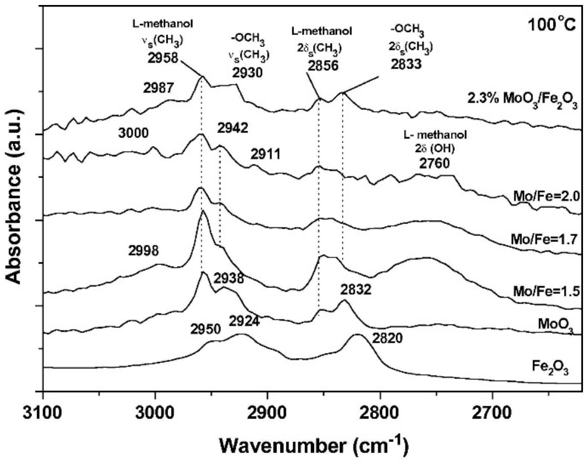

Figure 2. *In situ* CH_3OH-IR spectra after methanol chemisorption at 100°C on bulk Fe_2O_3, MoO_3 iron molybdates (Mo/Fe = 1.5, 1.7 and 2.0) and supported 2.3% MoO_3/Fe_2O_3 (complete monolayer of surface MoO_x) catalysts. Reproduced from ref. [27] with permission.

There is only one reported study, to the best of my knowledge, where methanol titration was applied to count the number of surface sites to normalize the reaction rate for a reaction other than methanol oxidation [72]. The number of surface redox sites was determined by H_2CO/CH_3OH-TPSR to quantify the TOF_{redox} for propane ammoxidation at 420°C ($C_3H_8/O_2/NH_3$ = 9.8/25/8.6) by unsupported $VSbO_4$ and supported V-Sb-O/Al_2O_3 catalysts. The resulting TOF_{redox} values towards C_3 products (acrylonitrile and propylene) differed by only a factor of ~2. These findings demonstrate that (*i*) methanol chemisorption/temperature programmed surface reaction can be used to selectively count the number of active surface redox sites and (*ii*) the redox TOF values for corresponding unsupported and supported mixed oxides are rather similar.

Acid sites. The bulk ZrO_x-WO_x mixed oxide contains submonolayer surface ZrO_x sites on WO_3 particles that possesses extremely strong Brønsted acid sites that yield a methanol dehydration TOF_{acid} of ~2 x 10^{-1} s^{-1} at 300°C [73]. This TOF_{acid} is an order of magnitude greater than that for a monolayer of surface WO_x sites on ZrO_2 at the same reaction temperature (~1 x 10^{-2} s^{-1}). The enhanced acidity of the bulk ZrO_x-WO_x mixed oxide is related to the presence of sub-monolayer surface ZrO_x sites on the surface of the WO_3 nanoparticles that increase the Brønsted acidity by lowering the deprotonation energy. The actual TOF_{acid} value of these superactive acid sites is probably greater by a factor of ~10^1-10^2 since the total number of sites used in determining the TOF also included all surface WO_x sites in the catalyst (both superactive and modestly active sites).

(ii) **Coverage of surface enriched oxide forms a complete monolayer.**

Redox sites. Methanol chemisorption on the stoichiometric bulk $FeVO_4$ mixed oxide only exhibits IR bands from surface species coordinated at surface VO_x sites, with V-OCH_3 >> V-CH_3OH, indicating monolayer surface VO_x coverage [74]. The IR vibrational differences between the surface Fe-OCH_3 (2924 and 2820 cm^{-1})/Fe-CH_3OH (2950 and 2850 cm^{-1}) and V-OCH_3 (2930 and 2828 cm^{-1})/V-CH_3OH (2962 and 2854 cm^{-1}) species differ by ~6-12 cm^{-1} allowing discrimination between the species coordinated to exposed VO_x and FeO_x sites. Methanol chemisorption on the stoichiometric bulk crystalline $FeVO_4$ mixed oxide phase gives the total number of active sites as 0.6 x 10^{15} sites/cm^2 and a TOF_{redox} of 0.05 s^{-1} for methanol oxidation at 230°C. Although the isotropic $FeVO_4$ crystalline phase exhibits ~4.5x higher surface density of surface VO_x sites than the active sites on the anisotropic V_2O_5 crystalline phase, the methanol oxidation TOF_{redox} values at 230°C for both catalysts are quite similar (0.05 s^{-1} for $FeVO_4$ and 0.03 s^{-1} for V_2O_5) as well as their Tp values of 200/201°C during CH_3OH-TPSR. This example is consistent with the earlier conclusion that the enhanced catalytic activity of mixed oxides compared to their anisotropic pure oxide counterparts is primarily related to their higher surface density of active sites. It would not have been possible to make such a reactivity comparison between the two catalysts without knowledge of the number of active surface sites showing that both mixed oxide catalysts have almost identical TOF values.

Acid Sites. Co-precipitation of aqueous $(NH_4)10W_{12}O_{41}\cdot 5H_2O$ and $ZrO_x(OH)_{4-2x}$ forms crystalline ZrO_2 with mostly surface enriched WO_x sites and some Zr-WO_3 NPs [72]. Comparison of methanol dehydration by the co-precipitated WO_x/ZrO_2 and model impregnated WO_x/ZrO_2 monolayer catalyst at 300°C revealed that at monolayer coverage the TOF_{acid} for the co-precipitated catalyst (5 x 10^{-2} s^{-1}) is more than an order of magnitude greater than the model WO_x/ZrO_2 catalyst (3 x 10^{-3} s^{-1}). The enhanced activity of the co-precipitated catalyst is a consequence of the presence of some superactive Zr-WO_3 NPs at monolayer coverage resulting from the co-precipitation synthesis.

(iii) **Coverage of surface enriched oxide exceeds monolayer.**

Redox sites. Increasing the MoO_x content of bulk iron molybdate catalysts above the stoichiometric Mo/Fe = 1.5 value results in the formation of crystalline MoO_3 NPs residing on top of the surface MoO_x monolayer present on the crystalline $Fe_2(MoO_4)_3$ phase. These crystalline MoO_3 NPs are readily detected by Raman spectroscopy [27]. The weak *in situ* IR bands from surface Fe-OCH_3 species are not present (see Figure 2) and LEIS surface analysis independently confirms that there are no exposed Fe sites in the outermost surface layer. The synthesis of bulk iron molybdate catalysts above stoichiometric Mo/Fe = 1.5 decreases the BET specific surface area, but increases the surface density of the number of redox active sites by a factor of ~2x that results in essentially the same TOF_{redox} values for methanol oxidation at 230°C (0.04 s^{-1}). The excess MoO_3 primarily serves as a reservoir to replace volatile MoO_x sites, via formation of Mo-OCH_3, to maintain a complete monolayer of surface MoO_x sites that increases the redox HCHO selectivity because of the absence of exposed acidic Fe sites responsible for unselective DME formation. This demonstrates that the surface MoO_x sites dominate the methanol oxidation reaction by bulk iron molybdate catalysts independent of the bulk Mo/Fe ratio (1.5 < Mo/Fe < 2.0)

Acid sites. Co-precipitation of aqueous $(NH_4)10W_{12}O_{41}\cdot5H_2O$ and $ZrO_x(OH)_{4-2x}$ with excess tungsten oxide yields a crystalline ZrO_2 phase with surface enriched WO_x sites and Zr-WO_3 NPs [72]. For the model supported WO_x/ZrO_2 catalyst with excess tungsten oxide, both a surface WO_x monolayer and crystalline WO_3 NPs are present. Comparison of methanol dehydration by the co-precipitated WO_x/ZrO_2 and model impregnated WO_x/ZrO_2 catalyst above monolayer coverage (~7 W/nm^2) at 300°C revealed that the TOF_{acid} for the co-precipitated catalyst (7 x 10^{-1} s^{-1}) is more than two orders of magnitude greater than the model WO_x/ZrO_2 catalyst (4 x 10^{-3} s^{-1}). The enhanced activity of the co-precipitated catalyst at slightly above monolayer coverage is a consequence of the presence of superactive Zr-WO_3 NPs resulting from the co-precipitation synthesis that are absent for the model impregnated supported WO_x/ZrO_2 catalyst [72].

Of all the types of oxide catalysts, application of methanol chemisorption is anticipated to have the biggest impact on unsupported, bulk mixed oxides since the number of active surface sites (Ns) that are present for such catalysts have been rarely reported. This has prevented determination of TOF values that would allow comparing the intrinsic activities of different catalysts and the influence of synthesis method, effect of composition, role of co-cations, influence of particle size, effect of exposed surface planes, etc. Knowledge of Ns will provide TOF values that will allow comparison of the TOF values for bulk mixed oxides, supported metal oxides and pure oxides of containing similar elements. Furthermore, with the aid of *in situ* IR spectroscopy, the nature of the coordination sites and elemental surface composition can be determined when the exposed cations give rise to different vibrations. Application of the methanol chemisorption approach should be a game changer for the catalysis science of bulk mixed oxide catalysts.

3. Conclusions and Future Directions

Methanol chemisorption has emerged as the ideal chemical probe for determining the number of active surface sites for all types of oxide catalysts, however, to date has primarily been employed for methanol reactions. The use of methanol chemisorption to count number of surface sites of oxide catalysts should also be applicable for normalizing non-methanol reactions as was demonstrated for propylene ammoxidation by bulk $VSbO_4$ and supported VO_x-SbO_x/Al_2O_3 mixed oxide catalysts. The typical number of active surface sites on isotropic one component oxides as probed by methanol is found to be ~0.7 x 10^{15} sites/cm^2, which is about half of that for metals (~1.2 x 10^{15} sites/cm^2) because the surface density of sites on oxides is less than on metals. The number of active surface sites on anisotropic oxides (MoO_3, V_2O_5 and ZnO) is significantly lower (~0.1 x 10^{15}/cm^2) because of the presence of much less active exposed surface planes related to the presence of coordinatively saturated sites. Knowledge of the Ns values allowed determining the TOF_{redox} and TOF_{acid} values for reactions by oxide catalysts. For pure oxides (one-component), the TOF values varies ~10^7x for redox sites and ~10^3x for acid sites indicating the ability to control the specific catalytic activity over an extremely wide range. For supported oxides, the active surface oxide sites generally control the TOF value in the sub-monolayer region. Above monolayer surface coverage, the crystalline MO_x nanoparticles decrease the available exposed surface MO_x sites. For redox sites, the crystalline MO_x nanoparticles have a minimal contribution to the TOF_{redox} value. For acid sites, the crystalline MO_x nanoparticles significantly increased the TOF_{acid} value. The crystalline bulk mixed oxide catalysts were found to be surface enriched in the MO_x active components. For redox sites, the surface MO_x sites dominated the TOF_{redox} above monolayer coverage. For acid sites, the crystalline MO_x nanoparticles dominated the TOF_{acid} above monolayer coverage because of the increased Brønsted acidity associated with the acidic nanoparticles. For redox catalysts, the TOF_{redox} values for supported oxides and their corresponding bulk mixed oxides have been found to be very similar given their common coordinating ligand (e.g., MoO_3/Fe_2O_3 and $Fe_2(MoO_4)_3$). For acid catalysts, the TOF_{acid} values for supported oxides (WO_3/ZrO_2) and their corresponding bulk mixed oxides (e.g., Zr-WO_3) are found to be very different with the bulk mixed oxides much more active. For redox oxide catalysts, most of the emphasis to date has been on molybdates and vanadates and future studies need to further expand the data base and extend studies to other redox cations (e.g., chromates, rhenates, etc.). For acid oxide catalysts, the cation that has been mostly investigated has been tungsta and it is, therefore, vital to investigate additional bulk tungstate mixed oxides and to also extend studies to other acidic cations (e.g., niobates, aluminates, etc.).

The methodology already exists to determine Ns and TOF values for oxide catalysts with methanol chemisorption, but the catalysis community has not rigorously adopted it. Such an adoption by the catalysis community will allow catalysis by oxides to be raised to the same catalysis science level as catalysis by metals that was initiated in the 1970s when chemisorption methods were developed to determine Ns values for metals. This would finally allow comparison of TOF values for different oxide catalysts and among laboratories. Only when such an extensive data base becomes available will it be possible to make fundamental conclusions about oxide catalysis (influence of synthesis method, effect of composition, role of co-cations, influence of particle size, effect of exposed surface planes, etc.). Additionally, the knowledge of TOF values would allow examining proposed hypotheses in the literature and establishing new concepts.

Acknowledgements

This article was inspired by Professor Michel Boudart who impressed upon me during my graduate studies at Stanford University the importance of the number of active surface sites and TOF values for catalysis by metals.

The writing of this article was supported as part of the Center for Understanding and Control of Acid Gas-Induced Evolution of Materials for Energy (UNCAGE ME), an Energy Frontier Research Center funded by the U.S. Department of Energy, Office of Science, Basic Energy Sciences under award # DE-SC0012577. Special thanks to Drs. M.E. Ford and B. Mosevitzky Lis for their input of this article.

References

[1] C.L. Thomas, Catalytic Processes and Proven Catalysts, Academic Press, New York, 1970.
[2] W.L. Holstein, C.J. Machiels, Inhibition of Methanol Oxidation by Water Vapor—Effect on Measured Kinetics and Relevance to the Mechanism, J. Catal. 162 (1996) 118–124. https://doi.org/10.1006/jcat.1996.0265.
[3] M.A. Bañares, Supported metal oxide and other catalysts for ethane conversion: a review,

Catal. Today. 51 (1999) 319–348. https://doi.org/10.1016/S0920-5861(99)00053-X.
[4] D. Siew Hew Sam, V. Soenen, J.C. Volta, Oxidative dehydrogenation of propane over V-Mg-O catalysts, J. Catal. 123 (1990) 417–435. https://doi.org/10.1016/0021-9517(90)90139-B.
[5] R.K. Grasselli, J.D. Burrington, D.J. Buttrey, P. Desanto, C.G. Lugmair, A.F. Volpe, T. Weingand, Multifunctionality of active centers in (amm)oxidation catalysts: from Bi–Mo–Ox to Mo–V–Nb–(Te, Sb)–Ox, Top. Catal. 23 (2003) 5–22.
[6] G. Centi, F. Trifiro, J.R. Ebner, V.M. Franchetti, Mechanistic aspects of maleic anhydride synthesis from C4 hydrocarbons over phosphorus vanadium oxide, Chem. Rev. 88 (1988) 55–80. https://doi.org/10.1021/cr00083a003.
[7] M.S. Wainwright, N.R. Foster, Catalysts, Kinetics and Reactor Design in Phthalic Anhydride Synthesis, Catal. Rev. 19 (1979) 211–292. https://doi.org/10.1080/03602457908068056.
[8] A. Urbanek, M. Trela, Catalytic Oxidation of Sulfur Dioxide, Catal. Rev. 21 (1980) 73–133. https://doi.org/10.1080/03602458008068061.
[9] J.P. Dunn, H.G. Stenger, I.E. Wachs, Molecular structure–reactivity relationships for the oxidation of sulfur dioxide over supported metal oxide catalysts, Catal. Today. 53 (1999) 543–556. https://doi.org/10.1016/S0920-5861(99)00142-X.
[10] H. Bosch, F. Janssen, Catalytic reduction of nitrogen oxides – a review on the fundamentals and technology: Catalyst testing, Catal. Today. 2 (1988) 403–431. https://doi.org/10.1016/0920-5861(88)80004-X.
[11] J.C. Vartuli, J.G. Santiesteban, P. Traverso, N. Cardona-Martinéz, C.D. Chang, S.A. Stevenson, Characterization of the Acid Properties of Tungsten/Zirconia Catalysts Using Adsorption Microcalorimetry and n-Pentane Isomerization Activity, J. Catal. 187 (1999) 131–138. https://doi.org/10.1006/jcat.1999.2595.
[12] M. Zhang, Y. Yu, Dehydration of Ethanol to Ethylene, Ind. Eng. Chem. Res. 52 (2013) 9505–9514. https://doi.org/10.1021/ie401157c.
[13] J.M. Thomas, W.J. Thomas, Principles and Practice of Heterogeneous Catalysis, VCH: Weinheim, Germany, 1997.
[14] S. Saravanamurugan, M. Palanichamy, B. Arabindoo, V. Murugesan, Solvent free synthesis of chalcone and flavanone over zinc oxide supported metal oxide catalysts, Catal. Commun. 6 (2005) 399–403. https://doi.org/10.1016/j.catcom.2005.03.005.
[15] V. Crocellà, G. Cerrato, G. Magnacca, C. Morterra, F. Cavani, S. Cocchi, S. Passeri, D. Scagliarini, C. Flego, C. Perego, The balance of acid, basic and redox sites in Mg/Me-mixed oxides: The effect on catalytic performance in the gas-phase alkylation of m-cresol with methanol, J. Catal. 270 (2010) 125–135. https://doi.org/10.1016/j.jcat.2009.12.011.
[16] M.M. Ostromecki, L.J. Burcham, I.E. Wachs, N. Ramani, J.G. Ekerdt, The influence of metal oxide additives on the molecular structures of surface tungsten oxide species on alumina: I. Ambient conditions, J. Mol. Catal. A Chem. 132 (1998) 43–57. https://doi.org/10.1016/S1381-1169(97)00226-4.
[17] I.E. Wachs, Recent conceptual advances in the catalysis science of mixed metal oxide catalytic materials, Catal. Today. 100 (2005) 79–94. https://doi.org/10.1016/j.cattod.2004.12.019.
[18] M. Boudart, G. Djéga-Mariadassou, Kinetics of Heterogeneous Catalytic Reactions, Princeton University Press, Princeton, 1984.
[19] B.M. Reddy, K.V.R. Chary, B.R. Rao, V.S. Subrahmanyam, C.S. Sunandana, N.K. Nag,

ESR, oxygen chemisorption and activity studies on MoO3-ZrO2 catalysts, Polyhedron. 5 (1986) 191–194. https://doi.org/10.1016/S0277-5387(00)84907-4.
[20] B.M. Reddy, B. Manohar, E.P. Reddy, Oxygen chemisorption on titania-zirconia mixed oxide supported vanadium oxide catalysts, Langmuir. 9 (1993) 1781–1785. https://doi.org/10.1021/la00031a028.
[21] G. Djéga-Mariadassou, L. Davignon, A.R. Marques, Dehydrogenation of propan-2-ol on zinc oxide powders as a structure-insensitive reaction, J. Chem. Soc. Faraday Trans. 1 Phys. Chem. Condens. Phases. 78 (1982) 2447. https://doi.org/10.1039/f19827802447.
[22] W.E. Farneth, F. Ohuchi, R.H. Staley, U. Chowdhry, A.W. Sleight, Mechanism of partial oxidation of methanol over molybdenum(VI) oxide as studied by temperature-programmed desorption, J. Phys. Chem. 89 (1985) 2493–2497. https://doi.org/10.1021/j100258a014.
[23] W.E. Farneth, R.H. Staley, A.W. Sleight, Stoichiometry and structural effects in alcohol chemisorption temperature-programmed desorption on molybdenum trioxide, J. Am. Chem. Soc. 108 (1986) 2327–2332. https://doi.org/10.1021/ja00269a031.
[24] W.E. Farneth, E.M. McCarron, A.W. Sleight, R.H. Staley, A comparison of the surface chemistry of two polymorphic forms of molybdenum trioxide, Langmuir. 3 (1987) 217–223. https://doi.org/10.1021/la00074a013.
[25] G. Busca, Infrared studies of the reactive adsorption of organic molecules over metal oxides and of the mechanisms of their heterogeneously-catalyzed oxidation, Catal. Today. 27 (1996) 457–496. https://doi.org/10.1016/0920-5861(95)00162-X.
[26] L.J. Burcham, L.E. Briand, I.E. Wachs, Quantification of Active Sites for the Determination of Methanol Oxidation Turn-over Frequencies Using Methanol Chemisorption and in Situ Infrared Techniques. 1. Supported Metal Oxide Catalysts, Langmuir. 17 (2001) 6164–6174. https://doi.org/10.1021/la010009u.
[27] K. Routray, W. Zhou, C.J. Kiely, W. Grünert, I.E. Wachs, Origin of the synergistic interaction between MoO3 and iron molybdate for the selective oxidation of methanol to formaldehyde, J. Catal. 275 (2010) 84–98. https://doi.org/10.1016/j.jcat.2010.07.023.
[28] M. Daturi, C. Binet, J.-C. Lavalley, A. Galtayries, R. Sporken, Surface investigation on CexZr1-xO2 compounds, Phys. Chem. Chem. Phys. 1 (1999) 5717–5724. https://doi.org/10.1039/a905758g.
[29] L.E. Briand, W.E. Farneth, I.E. Wachs, Quantitative determination of the number of active surface sites and the turnover frequencies for methanol oxidation over metal oxide catalysts: I. Fundamentals of the methanol chemisorption technique and application to monolayer supported molybdenum oxid, Catal. Today. 62 (2000) 219–229. https://doi.org/10.1016/S0920-5861(00)00423-5.
[30] M. Nagao, T. Morimoto, Adsorption of alcohols on zinc oxide surfaces, J. Phys. Chem. 84 (1980) 2054–2058. https://doi.org/10.1021/j100453a011.
[31] T. Morimoto, M. Kiriki, M. Nagao, Differential heat of chemisorption. 4. Chemisorption of methanol and 1-propanol on zinc oxide, J. Phys. Chem. 84 (1980) 2058–2061. https://doi.org/10.1021/j100453a012.
[32] R.N. Spitz, J.E. Barton, M.A. Barteau, R.H. Staley, A.W. Sleight, Characterization of the surface acid-base properties of metal oxides by titration/displacement reactions, J. Phys. Chem. 90 (1986) 4067–4075. https://doi.org/10.1021/j100408a047.
[33] R.P. Groff, An infrared study of methanol and ammonia adsorption on molybdenum trioxide, J. Catal. 86 (1984) 215–218. https://doi.org/10.1016/0021-9517(84)90363-4.

[34] F. Ohuchi, L.E. Firment, U. Chowdhry, A. Ferretti, Summary Abstract: Adsorption and temperature programmed desorption of methanol on MoO 3 powder and crystal surfaces, J. Vac. Sci. Technol. A Vacuum, Surfaces, Film. 2 (1984) 1022–1023. https://doi.org/10.1116/1.572664.
[35] G. Busca, P.F. Rossi, V. Lorenzelli, M. Benaissa, J. Travert, J.-C. Lavalley, Microcalorimetric and Fourier transform infrared spectroscopic studies of methanol adsorption on alumina, J. Phys. Chem. 89 (1985) 5433–5439. https://doi.org/10.1021/j100271a024.
[36] S.H. Liang, I.D. Gay, Adsorption and thermal decomposition of methanol on magnesium oxide. Carbon-13 NMR studies, Langmuir. 1 (1985) 593–599. https://doi.org/10.1021/la00065a014.
[37] P.F. Rossi, G. Busca, Microcalorimetric and FT-IR spectroscopic study of the adsorption of methanol on TiO2 (anatase), Colloids and Surfaces. 16 (1985) 95–102. https://doi.org/10.1016/0166-6622(85)80244-4.
[38] K.S. Kim, M.A. Barteau, W.E. Farneth, Adsorption and decomposition of aliphatic alcohols on titania, Langmuir. 4 (1988) 533–543. https://doi.org/10.1021/la00081a007.
[39] S. Kittaka, T. Umezu, H. Ogawa, H. Maegawa, T. Takenaka, Interaction of alcohols with surface hydroxyls on chromium(III) oxide, Langmuir. 14 (1998) 832–838. https://doi.org/10.1021/la970969+.
[40] A. Badri, C. Binet, J.-C. Lavalley, Use of methanol as an IR molecular probe to study the surface of polycrystalline ceria, J. Chem. Soc. Faraday Trans. 93 (1997) 1159–1168. https://doi.org/10.1039/a606628c.
[41] D. Bianchi, T. Chafik, M. Khalfallah, S. Teichner, Intermediate species on zirconia supported methanol aerogel catalysts V. Adsorption of methanol, Appl. Catal. A Gen. 123 (1995) 89–110. https://doi.org/10.1016/0926-860X(94)00242-8.
[42] A. Dahal, N.G. Petrik, Y. Wu, G.A. Kimmel, F. Gao, Y. Wang, Z. Dohnálek, Adsorption and Reaction of Methanol on Anatase TiO2(101) Single Crystals and Faceted Nanoparticles, J. Phys. Chem. C. 123 (2019) 24133–24145. https://doi.org/10.1021/acs.jpcc.9b07080.
[43] Y. Wu, F. Gao, H. Wang, L. Kovarik, B. Sudduth, Y. Wang, Probing Acid–Base Properties of Anatase TiO2 Nanoparticles with Dominant {001} and {101} Facets Using Methanol Chemisorption and Surface Reactions, J. Phys. Chem. C. 125 (2021) 3988–4000. https://doi.org/10.1021/acs.jpcc.0c11107.
[44] A.G. Pelmenschikov, G. Morosi, A. Gamba, A. Zecchina, S. Bordiga, E.A. Paukshtis, Mechanisms of methanol adsorption on silicalite and silica: IR spectra and ab-initio calculations, J. Phys. Chem. 97 (1993) 11979–11986. https://doi.org/10.1021/j100148a023.
[45] J. Cortes, M. Jensen, P. Araya, The adsorption of methanol on hydrophilic, hydrophobic and mixed silicas, J. Chem. Soc. Faraday Trans. 1 Phys. Chem. Condens. Phases. 82 (1986) 1351. https://doi.org/10.1039/f19868201351.
[46] C. Morterra, G. Magnacca, V. Bolis, On the critical use of molar absorption coefficients for adsorbed species: the methanol/silica system, Catal. Today. 70 (2001) 43–58. https://doi.org/10.1016/S0920-5861(01)00406-0.
[47] M. Badlani, I.E. Wachs, Methanol: A “Smart” Chemical Probe Molecule, Catal. Letters. 75 (2001) 137–149. https://doi.org/10.1023/A:1016715520904.
[48] S.E. Collins, L.E. Briand, L.A. Gambaro, M.A. Baltanás, A.L. Bonivardi, Adsorption and

Decomposition of Methanol on Gallium Oxide Polymorphs, J. Phys. Chem. C. 112 (2008) 14988–15000. https://doi.org/10.1021/jp801252d.
[49] B. Moulin, L. Oliviero, P. Bazin, M. Daturi, G. Costentin, F. Maugé, How to determine IR molar absorption coefficients of co-adsorbed species? Application to methanol adsorption for quantification of MgO basic sites, Phys. Chem. Chem. Phys. 13 (2011) 10797. https://doi.org/10.1039/c0cp02767g.
[50] C. Machiels, A.W. Sleight, Kinetic isotope effect in the selective oxidation of methanol to formaldehyde over some molybdate catalysts, J. Catal. 76 (1982) 238–239. https://doi.org/10.1016/0021-9517(82)90254-8.
[51] D. Fein, I.E. Wachs, Quantitative Determination of the Catalytic Activity of Bulk Metal Oxides for Formic Acid Oxidation, J. Catal. 210 (2002) 241–254. https://doi.org/10.1006/jcat.2002.3683.
[52] W.M.H. Sachtler, N.H. De Boer, Proc. 3rd Int. Congr. Catal., in: Wiley, Amsterdam, 1965: p. 240.
[53] B.A. Kazanskv, Proc. 4th Int. Congr. Catal., in: W.M.H. Sachtler, G.J.H. Dorgelo, J. Fahrenfort, R.J.H. Voorhoeve (Eds.), Adler, Moscow, 1968: p. 454.
[54] G.K. Boreskov, Catalytic Activation of Dioxygen, in: J.R. Anderson, M. Boudart (Eds.), Catal. Sci. Technol. Vol. 3, Springer Berlin Heidelberg, 1982: p. 62. https://doi.org/10.1007/978-3-642-93223-6_2.
[55] D. Kulkarni, I.E. Wachs, Isopropanol oxidation by pure metal oxide catalysts: Number of active surface sites and turnover frequencies, Appl. Catal. A Gen. 237 (2002) 121–137. https://doi.org/10.1016/S0926-860X(02)00325-3.
[56] J.-M. Jehng, H. Hu, X. Gao, I.E. Wachs, The dynamic states of silica-supported metal oxide catalysts during methanol oxidation, Catal. Today. 28 (1996) 335–350. https://doi.org/10.1016/S0920-5861(96)00047-8.
[57] W. Zhou, N. Soultanidis, H. Xu, M.S. Wong, M. Neurock, C.J. Kiely, I.E. Wachs, Nature of Catalytically Active Sites in the Supported WO3/ZrO2 Solid Acid System: A Current Perspective, ACS Catal. 7 (2017) 2181–2198. https://doi.org/10.1021/acscatal.6b03697.
[58] N. Vaidyanathan, D.M. Hercules, M. Houalla, Surface characterization of WO3/ZrO2 catalysts, Anal. Bioanal. Chem. 373 (2002) 547–554. https://doi.org/10.1007/s00216-002-1386-8.
[59] X. Gao, J.L.G. Fierro, I.E. Wachs, Structural Characteristics and Catalytic Properties of Highly Dispersed ZrO2/SiO2 and V2O5/ZrO2/SiO2 Catalysts, Langmuir. 15 (1999) 3169–3178. https://doi.org/10.1021/la981254p.
[60] X. Gao, S.R. Bare, J.L.G. Fierro, I.E. Wachs, Structural Characteristics and Reactivity/Reducibility Properties of Dispersed and Bilayered V2O5/TiO2/SiO2 Catalysts, J. Phys. Chem. B. 103 (1999) 618–629. https://doi.org/10.1021/jp983357m.
[61] X. Gao, I.E. Wachs, Structural Characteristics and Reactivity Properties of Highly Dispersed Al2O3/SiO2 and V2O5/Al2O3/SiO2 Catalysts, J. Catal. 192 (2000) 18–28. https://doi.org/10.1006/jcat.2000.2822.
[62] E.L. Lee, I.E. Wachs, Surface chemistry and reactivity of well-defined multilayered supported M1Ox/M2Ox/SiO2 catalysts, J. Catal. 258 (2008) 103–110. https://doi.org/10.1016/j.jcat.2008.06.002.
[63] I.E. Wachs, Raman and IR studies of surface metal oxide species on oxide supports: Supported metal oxide catalysts, Catal. Today. 27 (1996) 437–455. https://doi.org/10.1016/0920-5861(95)00203-0.

[64] T. Kim, I.E. Wachs, CH3OH oxidation over well-defined supported V2O5/Al2O3 catalysts: Influence of vanadium oxide loading and surface vanadium–oxygen functionalities, J. Catal. 255 (2008) 197–205. https://doi.org/10.1016/j.jcat.2008.02.007.
[65] T. Kim, A. Burrows, C.J. Kiely, I.E. Wachs, Molecular/electronic structure–surface acidity relationships of model-supported tungsten oxide catalysts, J. Catal. 246 (2007) 370–381. https://doi.org/10.1016/j.jcat.2006.12.018.
[66] X. Wang, I.E. Wachs, Designing the activity/selectivity of surface acidic, basic and redox active sites in the supported K2O-V2O5/Al2O3 catalytic system, Catal. Today. 96 (2004) 211–222. https://doi.org/10.1016/j.cattod.2004.06.145.
[67] E.L. Lee, I.E. Wachs, Comparison of Catalytic Active Sites Present in Supported MOx/SiO2, MOx/AlOx/SiO2 and MOx/ZSM-5 Catalysts, in: I. Halasz (Ed.), Silica Silic. Mod. Catal., Transworld Research Network, Kerala, 2010: p. 375.
[68] A. Bielański, J. Datka, B. Gil, A. Małecka-Lubańska, A. Micek-Ilnicka, Sorption of methanol on tungstosilicic acid, Phys. Chem. Chem. Phys. 1 (1999) 2355–2360. https://doi.org/10.1039/a900515c.
[69] L.E. Briand, A.M. Hirt, I.E. Wachs, Quantitative Determination of the Number of Surface Active Sites and the Turnover Frequencies for Methanol Oxidation over Metal Oxide Catalysts: Application to Bulk Metal Molybdates and Pure Metal Oxide Catalysts, J. Catal. 202 (2001) 268–278. https://doi.org/10.1006/jcat.2001.3289.
[70] L.E. Briand, J.-M. Jehng, L. Cornaglia, A.M. Hirt, I.E. Wachs, Quantitative determination of the number of surface active sites and the turnover frequency for methanol oxidation over bulk metal vanadates, Catal. Today. 78 (2003) 257–268. https://doi.org/10.1016/S0920-5861(02)00350-4.
[71] L.J. Burcham, L.E. Briand, I.E. Wachs, Quantification of Active Sites for the Determination of Methanol Oxidation Turn-over Frequencies Using Methanol Chemisorption and in Situ Infrared Techniques. 2. Bulk Metal Oxide Catalysts, Langmuir. 17 (2001) 6175–6184. https://doi.org/10.1021/la010010t.
[72] M.O. Guerrero-Pérez, T. Kim, M.A. Bañares, I.E. Wachs, Nature of Catalytic Active Sites for Sb−V−O Mixed Metal Oxides, J. Phys. Chem. C. 112 (2008) 16858–16863. https://doi.org/10.1021/jp801701m.
[73] E.I. Ross-Medgaarden, W. V. Knowles, T. Kim, M.S. Wong, W. Zhou, C.J. Kiely, I.E. Wachs, New insights into the nature of the acidic catalytic active sites present in ZrO2-supported tungsten oxide catalysts, J. Catal. 256 (2008) 108–125. https://doi.org/10.1016/j.jcat.2008.03.003.
[74] K. Routray, W. Zhou, C.J. Kiely, I.E. Wachs, Catalysis Science of Methanol Oxidation over Iron Vanadate Catalysts: Nature of the Catalytic Active Sites, ACS Catal. 1 (2011) 54–66. https://doi.org/10.1021/cs1000569.